

Principal Components Analysis Preprocessing for Improved Classification Accuracies in Pattern-Recognition-Based Myoelectric Control

Levi J. Hargrove*, *Member, IEEE*, Guanglin Li, *Senior Member, IEEE*, Kevin B. Englehart, *Senior Member, IEEE*, and Bernard S. Hudgins, *Senior Member, IEEE*

Abstract—Information extracted from multiple channels of the surface myoelectric signal (MES) recording sites can be used as inputs to control systems for powered upper limb prostheses. For small, closely spaced muscles, such as the muscles in the forearm, the detected MES often contains contributions from more than one muscle, the contribution from each specific muscle being modified by the dispersive propagation through the volume conductor between the muscle and the detection points. In this paper, the measured raw MES signals are rotated by class-specific principal component matrices to spatially decorrelate the measured data prior to feature extraction. This “tunes” the data to allow a pattern recognition classifier to better discriminate the test motions. This processing technique was used to significantly ($p < 0.01$) reduce pattern recognition classification error for both intact limbed and transradial amputee subjects.

Index Terms—Amputee, electromyography (EMG), myoelectric, myoelectric signal (MES), pattern recognition, principal components analysis, prostheses, transradial.

I. INTRODUCTION

THE SURFACE myoelectric signal (MES) is an electrophysiological signal generated by muscular contraction that propagates along the length of skeletal muscle to detection points on the skin’s surface. The surface MES has been used as an input to powered prosthesis control systems for over 40 years [1]. The first clinically viable and simplest myoelectric controllers mapped the amplitude of the MES, measured over selected control muscles, to a DOF of the prosthesis [2]. Other forms of conventional myoelectric control systems include the

three-state amplitude controller [3], three-state rate-sensitive controller [4], and myo-pulse controller [5]. Any of these systems may be used in conjunction with body-powered harnesses, mechanical switches, and force-sensitive resistors as part of an overall conventional prosthesis control strategy. These systems work well in some cases, but the number of functions that can be restored and the intuitiveness of use are limited by the number of appropriate control muscles from which to measure the MES. It is interesting to note that direct proportional control, a control system based on that described by Koblinski *et al.* [2] is currently used in one of the most advanced upper limb prostheses implemented to date [6].

Information extracted from *patterns* contained in the MES can also be used for control purposes. Pattern-recognition-based myoelectric control systems operate on the assumption that at a given electrode location, the set of features describing the MES will be repeatable for a given state of muscle activation and will also be different from one state of activation to another [7]. The problem is then reduced to MES signal representation to describe the activity in the channel and discrimination/classification to differentiate between the different motions. Currently, pattern-recognition-based myoelectric control systems are limited to sequential control and have yet to find widespread clinical acceptance; however, they have the potential to control more DOFs than conventional control strategies because they do not require independent control sites for each controlled motion [8]. In fact, it has been suggested that temporal-spatial information contained within muscle crosstalk may implicitly add class discriminatory information [9].

The focus of this study will be on below-elbow limb replacement. It is estimated that there are 60 000 below-elbow amputees in the United States [10], with 90% of amputations caused by trauma [11]. A typical below-elbow-powered prosthesis is composed of a powered hand, and possibly a 1-DOF-powered wrist controlled by conventional myoelectric control strategies. A survey completed in 1996 identified control of more DOFs is the greatest desire for below-elbow amputees [12]. Pattern-recognition-based control systems are leading candidates to replace additional DOFs.

For small, closely spaced muscles like those in the forearm, the detected MES often contains contributions from more than one muscle; the contribution from each specific muscle being modified by the dispersive propagation through the volume conductor (the “tissue filter”) between the muscle and the detection points. If the control sites are not independent, the spatial

Manuscript received February 18, 2008; revised May 18, 2008. First published October 31, 2008; current version published May 22, 2009. This work was supported by the Natural Sciences and Engineering Research Council of Canada (NSERC) under Discovery Grant 171368-03 and Grant 217354-01 and by the New Brunswick Foundation for Innovation and the Atlantic Innovation Fund. *Asterisk indicates corresponding author.*

*L. J. Hargrove was with the Institute of Biomedical Engineering, University of New Brunswick, Fredericton, NB E3B 5A3, Canada. He is now with the Neural Engineering Center for Artificial Limb, Rehabilitation Institute of Chicago, Chicago IL 60611, and also with the Department of Physical Medicine and Rehabilitation, Northwestern University, Chicago IL, 60208, USA (e-mail: l-hargrove@northwestern.edu).

G. Li was with the Neural Engineering Center for Artificial Limbs, Rehabilitation Institute of Chicago, Chicago, IL 60611 USA, and also with the Department of Physical Medicine and Rehabilitation, Northwestern University, Chicago, USA. He is now with Shenzhen Institute of Advanced Technology, Chinese Academy of Sciences, China.

K. B. Englehart and B. S. Hudgins are with the Institute of Biomedical Engineering, University of New Brunswick, Fredericton, NB E3B 5A3, Canada.

Color versions of one or more of the figures in this paper are available online at <http://ieeexplore.ieee.org>.

Digital Object Identifier 10.1109/TBME.2008.2008171

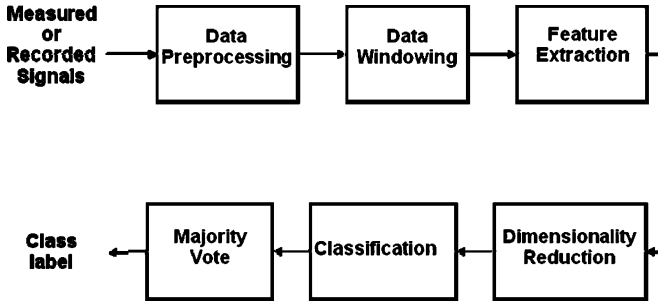


Fig. 1. Basic steps of pattern-recognition-based myoelectric control.

propagation of action potentials may yield correlated signals at different recording electrodes. This study introduces a set of motion-class-specific decorrelation filters based on principal components analysis (PCA) to spatially decorrelate the detected signals prior to feature extraction. It is hypothesized that the projections down the PCA transformation matrix of the intended class will enhance or “tune” the data while projections down the remaining PCA transformation matrices will not yield additional information. This method provides a method to explicitly use information contained in muscle crosstalk to significantly improve classification accuracy for both intact limbed and amputee subjects. The performance of the motion-class-specific PCA technique will be compared to a system that uses projections down a universal PCA matrix computed across all motion classes, and to a system that uses no PCA.

II. BACKGROUND

A. Myoelectric Control Terminology

Prior to further describing the control strategies, it is useful to provide some definitions that are often used in the field of myoelectric control for powered prostheses and will be used in the subsequent sections. An *MES control site* is the area on the surface of the skin above a muscle from which the MES signal is measured from. A *channel* of MES data refers to a bipolar measurement from electrodes located over top of a control site. A *feature* of the data refers to some descriptor of the measured signal over a given time window. A *DOF* is a rotation about a joint or coordinate axis. A *motion class* is any actuation that the prosthesis is capable of making in one direction along one or multiple DOFs. For example, elbow flexion and elbow extension are motion classes and form 1 DOF, which is rotation about the elbow joint. A motion class also includes preprogrammed, coordinated movements about multiple DOFs such as handgrips. *Proportional control* uses the amplitude from a control site in conventional control, or an average of the amplitudes across all channels in pattern recognition control to control the velocity of the actuated motion class.

B. Pattern-Recognition-Based Myoelectric Control

A generalized block diagram of myoelectric pattern recognition control is shown in Fig. 1. Data pre-preprocessing typically consists of MES amplification to a convenient value and band-pass filtering between approximately 20 and 500 Hz to remove motion artifacts. Sometimes, a notch filter is placed at 50 or

60 Hz to remove power line interference. Due to the random nature of the MES, the instantaneous value of the MES is not useful for control purposes. Consequently, data analysis windows must be formed from which features are extracted. The window must be short enough so that an excessive delay is not introduced to the controller, yet long enough that a reliable decision can be formed. Estimates for allowable data window lengths range from 50 ms [13] to 400 ms [14]; longer analysis windows yielding greater classification accuracies [15].

The feature extraction and classification portion of the pattern recognition system have been the subject of extensive research. Some commonly investigated feature sets include time domain (TD) features [15], autoregressive (AR) coefficients [7], cepstral coefficients [16], the short-time Fourier transform, the wavelet transform, the wavelet packet transform [17], and concatenated TD and AR (TDAR) [9] features. Certain feature sets, such as the wavelet packet transform, must be used in conjunction with dimensionality reduction such as PCA [17] or uncorrelated linear discriminant analysis (ULDA) [18], to overcome the “curse of dimensionality”¹ and yield proper signal representation [19]. Most modern classification methods have been investigated such as Bayesian classifiers [20], artificial neural networks [20], Gaussian mixture models [9], hidden Markov models [21], fuzzy logic [22], [23] and genetic algorithms [24]; however, they all yield similar results provided the MES is represented properly through a judicious choice of feature set [8]. If fast processors are used, a majority vote can be used to remove spurious misclassifications from the decision stream and ensure smooth transitions between motion classes [15]. The number of decisions that can be used in a majority vote depends upon the length of the analysis window, the system processing delay, and the total system delay tolerable by the user. For example, a 100-ms analysis window with a processing delay of 10 ms and a tolerable user delay of 250 ms could allow for a total of 15 decisions to be used in a majority vote scheme. The majority vote is simply the decision that occurs most frequently during the 15 decision majority vote queue. An intensity calculation composed of a linear combination of MES amplitude estimates can be used to provide proportional control [25].

C. Principle Components Analysis

PCA is an orthogonal linear transformation that decorrelates multivariate data and projects it onto a new coordinate system such that the greatest variance in the data lies on the first coordinate while the least variance in the data tends to lie on the last coordinate [26]. Given M observations of a N length random vector \bar{z} , the PCA transform is completed by first subtracting the mean from the vector

$$\bar{x} = \bar{z} - E[\bar{z}]. \quad (1)$$

The $N \times N$ covariance matrix C_x is computed

$$C_x = E[\bar{x}\bar{x}']. \quad (2)$$

¹The “curse of dimensionality” refers to an exponential increase in hypervolume as a function of dimensionality. Consequently, many more training samples are needed to populate the feature space for generic classification problems sufficiently.

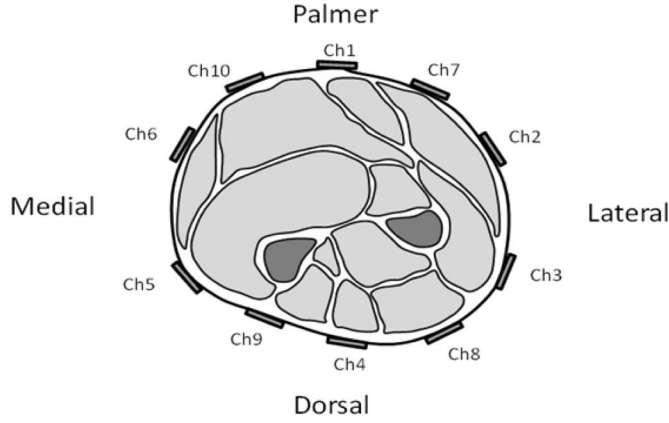


Fig. 2. Surface electrode placement on the forearm. Electrodes were placed longitudinally along the muscle fiber approximately one-third the distance between the forearm and wrist for intact limbed subjects.

The principal components \bar{s} of \bar{x} are given in terms of the unit-length eigenvectors $(\bar{e}_1 \cdots \bar{e}_N)$, of C_x

$$\bar{s} = W\bar{x}. \quad (3)$$

Where the projection matrix W contains the eigenvectors $(\bar{e}_1 \cdots \bar{e}_N)$. Usually the M observations would typically be exemplars taken from any one of C possible classes. This is termed universal PCA (uPCA) or global PCA [27]. This provides a means of unsupervised dimensionality reduction, as no class membership qualifies the data when specifying the eigenvectors of maximum variance within the covariance matrix.

A recent variation, termed individual PCA (iPCA) [28] or classwise PCA [29], groups the M observations by their class membership. Separate projection matrices $W_1 \cdots W_C$ are found for each class. This method effectively “tunes” the data prior to classification and has been shown to improve classification accuracies for some pattern recognition problems.

III. METHODS

A. Experimental Protocol

MES data corresponding to 11 motion classes were collected from ten healthy subjects and five long traumatic transradial amputees. Amputee data were collected at the Rehabilitation Institute of Chicago in an IRB approved experiment. Data from intact-limbed subjects were collected at the University of New Brunswick in an experiment approved by the University of New Brunswick’s Research Ethics Board.

Ten adhesive duotrodes² were placed on the proximal portion of the forearm as illustrated in Fig. 2. Twelve locations were marked at circumferentially equal lengths on the forearm, around the apex of the muscle bulge. The duotrodes were placed at ten of these markings, excluding the medial and lateral marking.

Experimental data were collected from subjects for eight trials. Each trial consisted of two repetitions of the following 11

types of motion classes performed in sequential order: wrist pronation/supination, wrist flexion/extension, hand open, key grip, chuck grip, power grip, fine pinch grip, tool grip, and a rest class. Note that the rest position is defined as one of the motion classes in this work, and the rest position for intact-limbed subjects was 0° flexion, with the palm of the hand perpendicular to the floor. The subject’s elbow was allowed to rest on an armrest. Amputee subjects completed the experiment with their elbow resting on an armrest. The subjects were not restrained in any way during data collection and were given instructions to elicit repeatable, constant-force contractions to the best of their ability. The intensity of the contraction was determined by the subject, but they were encouraged to contract to a level that they comfortable repeating for the duration of the experiment. Subjects were given approximately 10 min during which they could practice the series of contractions. During this time, the experimenter would instruct the subject to complete each of the desired contractions multiple times while observing the raw signals in real time until the experimenter felt the subject was making repeatable contractions. Furthermore, the MESs were examined by the experimenter to ensure that good electrode/skin was maintained for all motions and that the gains of the amplifiers were appropriately set to avoid saturation. During all trials, subjects elicited the contraction from the rest position, held the contraction for 4 s and then returned to the rest position for a predetermined inter-motion class delay period. Amputee subjects were encouraged to move their phantom limb in a repeatable fashion to the best of their ability. Trials 1, 2, 3, and 4, used intermotion class delay periods of 3, 2, 1, and 0 s, respectively. Note that a delay of 0 in trial 4 implies that the subjects transitioned between the motion classes for this trial. Trials 5–8 used intermotion class delay periods of 2 s. Each subject was given a brief rest period between trials to prevent fatigue. The rest period lasted at least 2 min; however, subjects were given additional rest if they felt tired. The entire experiment, including electrode placement, took less than 2 h to complete.

MES data recorded from trials 1–4, excluding the intermotion class delays, were used to create a set of training data. MES data recorded from trials 5 and 6 excluding inter-motion class delays were used as a validation set to perform channel reduction as described in Section III-B and MES data recorded from trials 7 and 8, excluding intermotion class delays were used as a test dataset. All data were collected using a custom built preamplification system, a 16-bit data acquisition (DAQ) and custom DAQ software, sampled at 1 kHz per channel.

B. Data Processing

There are many configuration options of the data windowing, feature extraction, dimensionality reduction, and classification blocks as noted in Section II-A. For this study, the baseline classification system was one that used an AR feature set, ULDA feature reduction, classified with an LDA classifier. No majority vote or proportional control estimate was computed. The remainder of this section will discuss the iPCA preprocessing block.

²Manufactured by 3M.

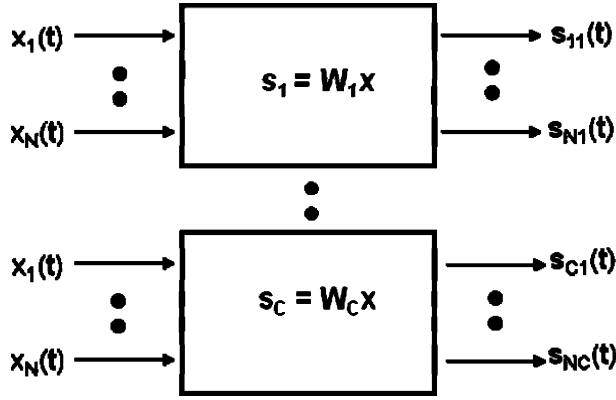


Fig. 3. Block diagram showing the iPCA tuning preprocessing block. This form of signal processing increases the dimensionality of the input by a factor of C where C is the total number of motion classes. The inputs to this block are x , the N channels of MES. The outputs of the channels are s , the linear projections down the C iPCA matrices.

For the described experiment, the measured MES can be considered a zero mean random variable

$$\bar{z}(\bar{m}) = \bar{x}(\bar{m}) = \begin{bmatrix} x_1(m) \\ \vdots \\ x_{10}(m) \end{bmatrix}, \quad m = 1, \dots, M \quad (4)$$

where M is the total number of discrete time *training* samples. If uPCA is used, M equates to 176 000 observations and the W_U can be found according to (1)–(3). When using iPCA, M is grouped by class so that $M_c = 16\,000$, $c = 1, \dots, 11$. The iPCA matrices W_c , can be computed according to (1)–(3). When iPCA is used, the algorithm simultaneously projects data down the iPCA transformation matrices prior to data windowing and feature extraction. Fig. 3 illustrates the completed iPCA algorithm block that may be inserted into “data preprocessing” location in the block diagram shown in Fig. 1.

Fig. 3 shows the iPCA tuning algorithm increases the dimensionality of the inputs by a factor of C , where C is the total number of classes. Real-time implementation of this algorithm would be challenging due to the high number of motion classes and channels under investigation. Furthermore, the high dimensionality requires a large training dataset to overcome the curse of dimensionality and allow the classifier to generalize well. A simple iterative sequential forward selection (SFS) algorithm was used to reduce the dimensionality of the data [30]. This algorithm iteratively adds the most informative linearly combined channel to a subset, as determined by the empirical classification performance of a validation set. The SFS algorithm was used to reduce the number of channels to 30 as this provided good classification accuracy.

A nine-motion-class system and seven-motion-class system were also investigated in addition to the 11-motion-class system. The seven-motion class contains: wrist pronation/supination, wrist flexion/extension, hand open, and power grip and rest. The nine-motion class subset contains all the motion classes in the seven-motion class subset plus key grip and chuck grip. The classification accuracy was computed for the 11-, 9-, and 7-motion class systems when six channels of MES (c1–c6) and

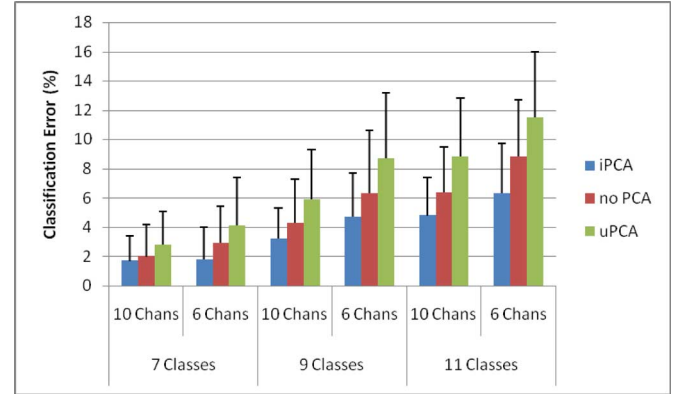


Fig. 4. Comparison of classification errors resulting from processing with and without PCA tuning, using intact limbed subjects. The error bar represents one standard deviation of intersubject variability.

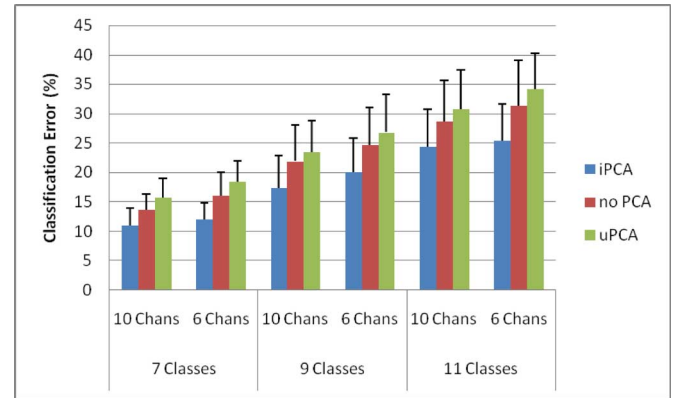


Fig. 5. Comparison of classification errors resulting from processing with and without PCA tuning, using amputee subjects. The error bar represents one standard deviation of intersubject variability.

ten channels of MES (c1–10) were used as input. The real-time performances of the various systems with and without the iPCA preprocessing algorithm were bench tested using MATLAB on a 3.0 GHz Intel Xeon 5160 Workstation.

IV. RESULTS

Fig. 4 displays the classification accuracies obtained from intact-limbed subjects for no PCA preprocessing (no PCA), uPCA preprocessing, and iPCA processing for 7-, 9-, and 11-motion-class problems and for each of the six and ten MES channel cases. Fig. 5 displays the classification accuracies obtained from amputees for the same situations.

A two-way analysis of variance (ANOVA) was performed on intact-limbed data and determined that in all cases, the iPCA preprocessing algorithm significantly outperforms systems without PCA preprocessing ($p < 0.01$) or with uPCA preprocessing ($p < 0.01$). Similarly, a two-way ANOVA was performed on amputee data and determined that in all cases the iPCA preprocessing algorithm significantly outperforms systems without PCA preprocessing ($p < 0.01$) or with uPCA preprocessing ($p < 0.01$). Fig. 6 displays the performance of each amputee subject for the six-channel, seven-motion-class control system.

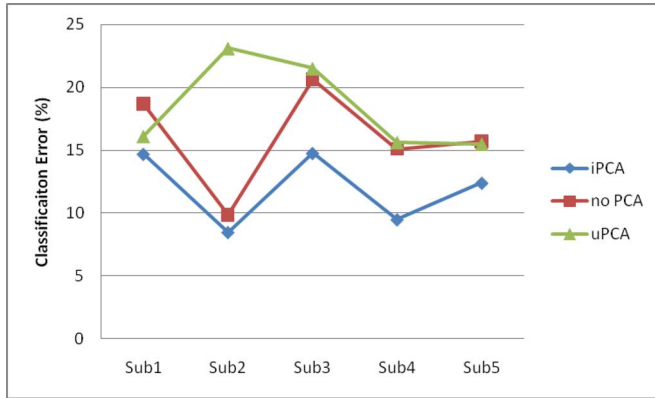


Fig. 6. Line-plot displaying the classification error for the six-channel, seven-class problem for amputees on a subject by subject basis.

Table I displays the average prediction performance across the five amputee subjects for the six-channel, seven-motion class problem while Table II displays the same information for the six-channel 11-motion class problem for intact-limbed subjects.

The results of bench testing determined that the complete decision processing time for the 10-channel, 11-motion-class pattern recognition system without preprocessing was determined to be 4 ms. This processing time increased to 12 ms when iPCA preprocessing was introduced.

V. DISCUSSION

Figs. 4 and 5 show that similar trends in classification errors exist between intact-limbed subjects and amputees. In all cases, the ten-channel-input case outperformed the six-channel-input case, and the classification errors increased with the number of desired classes to be controlled. These results were expected as more channels add information to the system, and more classes increase the complexity of the decision space. The six-channel case was included because it is difficult to embed ten electrode pairs into a prosthesis socket.

Figs. 4 and 5 show that the classification errors for amputees were much higher than for intact-limbed subjects. There may be a number of reasons for these differences. First is the lack of availability of musculature from which the MES can be measured. Even though this study focused on long transradial amputee subjects, they still lacked the complete musculature available from intact-limbed subjects. Furthermore, the residual limb muscles had not been exercised since the time of amputation and they had atrophied. A second possible reason why intact-limbed subjects performed better is that they had both proprioceptive and visual feedback. Feedback helps to make repeatable motions while amputees had no feedback and had to visualize moving their phantom limb. This is especially important when trying to differentiate between the grip types; intact-limbed subjects could watch to ensure that their hand is in the proper orientation while amputees had no feedback. A third possible reason why intact-limbed subjects performed better is that they were comfortable making the contractions under investigation and reported no fatigue. Amputee subjects were not used to of using their residual muscles, and reported some fatigue near the end

of the experiments. Over time, amputees could likely rebuild their musculature through training to overcome the fatigue issue. The training could also improve the repeatability of their patterns that would yield higher classification accuracies. Given the challenges listed above, the nine- and seven-motion class investigation was performed, as it was a more reasonable task for amputees to perform.

Fig. 6 displays the six-channel, seven-motion class system for amputee's on a subject-by-subject basis. All other control systems showed similar trends; iPCA preprocessing outperforms other preprocessing techniques in all cases for all subjects. It is interesting that uPCA yields lower classification accuracies than no PCA preprocessing. uPCA orders the components by the amount of variance each component explained and not by a discriminatory power. Thus it is not expected to result in classification accuracy improvement; however, it was not expected that it would yield lower accuracies.

PCA has been previously used as a signal processing technique for myoelectric control. PCA is often used with wavelets to reduce the number of features prior to classification [17]. Consequently, the principle components of the feature set were obtained. In the proposed algorithm the PCA is completed on the raw data prior to feature extraction. Micera *et al.* [31] used PCA on the raw MES to automatically determine which muscles were active and select appropriate electrodes prior to feature extraction; however, the muscles used were not as closely spaced as the muscles in the forearm.

The classification rates of amputee subjects do compare well with previous work using traumatic transradial amputees. Weir and Ajiboye [23] designed a fuzzy-logic-based classifier and were able to achieve 97% accuracy for a four-motion-class problem. Fukada *et al.* [32] tested two traumatic amputees and was able to achieve an average classification accuracy of 86% for the seven-motion-class case investigated in this experiment. Due to the small sample sizes a statistical comparison could not be completed.

The confusion matrices displayed in Tables I and II provide a direct comparison of a system using iPCA preprocessing versus a system with no preprocessing. It can be seen that iPCA preprocessing improves the classification accuracy across all motion classes with the exception of the rest class.

The relationship between classification accuracy and prosthesis controllability has yet to be clearly defined. A usability test needs to be completed to determine if the increased classification accuracy provided by the algorithm translates to increased controllability. Furthermore, a usability test will provide real-time feedback to amputee subjects in the form of the current state of activation of the prosthesis. This will allow them to identify misclassifications and attempt to compensate, potentially yielding higher classification accuracies.

The SFS is an attractive dimensionality reduction choice because after the appropriate channels have been chosen, the feed forward operation of the preprocessing algorithm reduces to

$$\bar{s} = \mathbf{W}_{\text{SFS}} \bar{x} \quad (5)$$

where \mathbf{W}_{SFS} is a 10×30 matrix and \bar{s} is the set of linearly mixed channels. Although the iterative SFS algorithm yields

TABLE I
CONFUSION MATRIX SHOWING THE DISTRIBUTION OF ERRORS FOR THE SIX-CHANNEL, SEVEN-CLASS PROBLEM FOR AMPUTEE SUBJECTS

	Pronation		Supination		Flex		Extend		Hand Open		Power Grip		Rest	
Pron.	88	89	0.7	0.3	2.6	0.8	0.0	0.9	0.6	0.3	0.4	0.6	7.6	7.4
Sup.	0.3	0.3	88	92	0.9	0.3	0.1	0.7	7.4	3.5	0.5	0.2	3.4	2.8
Flex.	0.9	0.9	3.4	2.0	94	94	0.0	0.0	0.6	0.4	0.5	1.7	1.0	0.9
Ext.	5.8	1.7	2.8	0.5	0.1	0.1	79	85	9.4	10.2	0.3	0.1	2.6	2.3
Hand Open	1.6	1.8	21.7	11.5	0.9	0.7	8.3	7.0	64	75	1.1	2.3	2.2	1.9
Power Grip	0.7	0.1	3.6	0.9	10.4	9.4	0.9	0.9	3.0	2.6	77	82	4.5	4.3
Rest	0.2	0.5	0.1	0.1	0.8	0.9	0.0	0.0	0.2	0.5	0.2	0.1	99	98

The values in white (left columns) show processing without iPCA tuning. The values in light gray (right columns) show the results with iPCA tuning and SFS data reduction. The results along the main diagonal (dark gray) are correct classifications (accuracy), and those lying outside of the main diagonal are incorrect classifications (error rate). Empty cells correspond to an error of 0%. The accuracies along the main diagonals are rounded to the nearest percent whereas the errors on the off diagonal are rounded to the nearest tenth of a percent.

TABLE II
CONFUSION MATRIX SHOWING THE DISTRIBUTION OF ERRORS FOR THE SIX-CHANNEL, 11-CLASS PROBLEM FOR INTACT LIMBED SUBJECTS

	Pronation		Supination		Flexion		Extension		Hand Open		Key Grip		Chuck Grip		Power Grip		Fine Pinch		Tool Grip		Rest	
Pron.	95	96			0.1				0.9	0.5	0.4	0.3	0.5	0.4	0.2	0.1	2.6	2.1	0.1	0.1	0.6	0.7
Sup.	0.1	0.0	97	98							0.4	0.1	0.2	0.2			1.2	0.4	0.1		0.8	0.9
Flex.	0.1		0.1	0.1	98	99						0.2	0.1	0.1	0.1	0.1	0.1		0.3	0.3	0.5	0.5
Ext.			0.1				98	98			0.1		0.3	0.5	0.1		1.3	0.9			0.4	0.3
Hand Open	5.2	4.8	0.2						88	92	0.5	0.1		0.3	0.0		4.9	1.0	0.6	0.5	0.5	0.4
Key Grip	0.0	0.0	0.1								80	85	5.3	4.6	9.7	8.8	3.3	0.9	0.9	0.2	0.9	0.4
Chuck Grip	0.9	0.4					0.1	0.1			3.5	2.6	89	93	1.1	0.4	3.8	2.4			1.6	0.7
Power Grip	0.3	0.1							0.1	0.1	5.9	3.8	2.1	1.7	90	92	0.2		0.9	2.3		
Fine Pinch	0.3						0.1		0.5	0.1	0.8	0.5	7.6	6.8	0.1	0.0	90	92	0.1	0.1	0.3	0.3
Tool Grip	0.2								3.1	2.6	4.1	3.1	0.3	0.5	6.3	3.7	0.7	0.2	85	90	0.4	
Rest	0.1				0.1				2.5	1.7	0.7	0.4	1.3	0.9	0.2		2.2	1.4			93	95

The values in white (left columns) show processing without iPCA tuning. The values in light gray (right columns) show the results with iPCA tuning and SFS channel reduction. The results along the main diagonal (dark gray) are correct classifications (accuracy), and those lying outside of the main diagonal are incorrect classifications (error rate). Empty cells correspond to an error of 0%. The accuracies along the main diagonals are rounded to the nearest percent whereas the errors on the off diagonal are rounded to the nearest tenth of a percent.

good results, a more robust method of data reduction is needed. As the algorithm is currently implemented, each channel was used, independently, to train and subsequently test classification performance. Consequently the SFS algorithm is highly dependent on the validation dataset. Different supervised and unsupervised data reduction techniques are currently being investigated to replace the SFS algorithm.

The AR + LDA classifier was chosen as the baseline classifier because previous work investigating similar motion classes has shown that this system significantly outperforms other feature sets and classifiers [8], [18]. A real-time embedded system has been developed using a Freescale MPC565 32 bit floating-point microcontroller, which is capable using 16 input channels to classify up to 25-motion classes in under 10 ms. The results of the real-time bench test indicate that the increase in processing time is directly related to the number of input channels from which features need to be extracted (4 ms for ten channels compared to 12 ms for the iPCA case that extracts features from 30 linearly mixed channels). Furthermore, iPCA preprocessing does not require significant additional memory requirements. Thus, it should be possible to implement iPCA preprocessing on a real-time embedded system within a reasonable time delay.

If one uses a very conservative estimate of a 50 ms total processing time to reach a decision, the described system can still make decisions within 200 ms (150 ms analysis window plus 50 ms processing time). This delay falls within the range of estimates for actuation of a powered prosthesis [13], [14], [33]. If a faster response time was desired, the analysis window could be shortened to make faster decisions at the expense of a slight degradation of classification performance.

As stated in Section I, pattern-recognition-based myoelectric control assumes that the state of muscle activation will not change and be repeatable. Small changes in the experimental conditions are unavoidable and will affect the detected state of muscle activation. To compensate for these changes, the experiments were kept short and gelled Ag-AgCl electrodes were used which provide good electrode impedance characteristics. The electrodes were observed carefully while the subjects completed the contractions to ensure sound skin/electrode contact was maintained. The topic of long-term pattern-recognition-based myoelectric control robustness is an active area of research. Clinical trials are ongoing to quantify how small signal changes impact pattern recognition over longer term use.

VI. CONCLUSION

A novel individual PCA tuning algorithm implementation was introduced for use with existing MES pattern-recognition-based prosthetic control systems. MES data were projected onto class-specific PCA transformation matrices for tuning, prior to pattern recognition classification. This processing technique was found to significantly reduce classification errors for both intact-limbed and amputee subjects. Future work will investigate real-time implementation of the algorithm followed by usability testing with feedback provided to the subjects.

ACKNOWLEDGMENT

The authors would like to thank Mr. E. Scheme for integration of the PCA turning algorithm into the University of New Brunswick (UNB) custom-built ACE software.

REFERENCES

- [1] P. Parker, K. Englehart, and B. Hudgins, "Myoelectric signal processing for control of powered prosthesis," *J. Electromyogr. Kinesiol.*, vol. 16, no. 6, pp. 541–548, Dec. 2006.
- [2] A. E. Koblinski, S. V. Bolkhovitin, L. M. Voskoboinikova, D. M. Ioffe, E. P. Polyan, B. P. Popov, Y. L. Slavutski, A. Y. Sysin, and Y. S. Yakobson, "Problems of bioelectric control," in *Proc. 1st IFAC Int. Congr. Autom. Remote Control*, J. F. Coles, Ed. London, U.K., 1960, vol. 2, pp. 619–623.
- [3] D. S. Dorcas and R. N. Scott, "A three-state myoelectric control," *Med. Biol. Eng.*, vol. 4, pp. 367–372, 1966.
- [4] D. A. Childress, "A myoelectric three state controller using rate sensitivity," in *Proc. 8th ICMBE*, Chicago, IL, 1969, pp. S4–S5.
- [5] D. S. Childress, "An approach to powered grasp," presented at the Fourth Int. Symp. External Control Hum. Extremities, Belgrade, Yugoslavia, 1973.
- [6] T. A. Kuiken, G. A. Dumanian, R. D. Lipschutz, L. A. Miller, and K. A. Stubblefield, "The use of targeted muscle reinnervation for improved myoelectric prosthesis control in a bilateral shoulder disarticulation amputee," *Prosthet. Orthot. Int.*, vol. 28, pp. 245–253, 2004.
- [7] D. Graupe, J. Salahi, and K. Kohn, "Multifunctional prosthesis and orthosis control via microcomputer identification of temporal pattern differences in single-site myoelectric signals," *J. Biomed. Eng.*, vol. 4, pp. 17–22, Jan. 1982.
- [8] L. J. Hargrove, K. Englehart, and B. Hudgins, "A comparison of surface and intramuscular myoelectric signal classification," *IEEE Trans. Biomed. Eng.*, vol. 54, no. 5, pp. 847–853, May 2007.
- [9] Y. H. Huang, K. Englehart, B. S. Hudgins, and A. D. C. Chan, "A Gaussian mixture model based classification scheme for myoelectric control of powered upper limb prostheses," *IEEE Trans. Biomed. Eng.*, vol. 52, no. 11, pp. 1801–1811, Nov. 2005.
- [10] "2000 Orthotics and prosthetics business and salary survey report," Amer. Orthot. Prosthet. Assoc. Alexandria, VA, 2000.
- [11] P. Owens and E. A. Ouellette, "Wrist disarticulation and transradial amputation: Surgical management," in *Atlas of Amputations and Limb Deficiencies*, 3rd ed., D. G. Smith, J. W. Michael, and J. H. Bowker, Eds. Rosemont, IL: American Academy of Orthopaedic Surgeons, 2004, pp. 219–222.
- [12] D. Atkins, D. C. Y. Heard, and W. H. Donovan, "Epidemiologic overview of individuals with upper-limb loss and their reported research priorities," *J. Prosthet. Orthot.*, vol. 8, pp. 2–11, 1996.
- [13] D. S. Childress and R. F. Weir, "Control of limb prostheses," in *Atlas of Amputations and Limb Deficiencies: Surgical, Prosthetic, and Rehabilitation Principles*, 3rd ed., D. G. Smith, J. W. Michael, and J. H. Bowker, Eds. Rosemont, IL: American Academy of Orthopaedic Surgeons, 2004, pp. 173–195.
- [14] G. Heffner, W. Zucchini, and G. G. Jaros, "The electromyogram (EMG) as a control signal for functional neuromuscular stimulation—Part I: Autoregressive modeling as a means of EMG signature discrimination," *IEEE Trans. Biomed. Eng.*, vol. 35, no. 4, pp. 230–237, Apr. 1988.
- [15] K. Englehart and B. Hudgins, "A robust, real-time control scheme for multifunction myoelectric control," *IEEE Trans. Biomed. Eng.*, vol. 50, no. 7, pp. 848–854, Jun. 2003.
- [16] W.-J. Kang, J.-R. Shiu, C.-K. Cheng, J.-S. Lai, H.-W. Tsao, and T.-S. Kuo, "The effect of electrode arrangement on spectral distance measures for discrimination of EMG signals," *IEEE Trans. Biomed. Eng.*, vol. 44, no. 10, pp. 1020–1023, Oct. 1997.
- [17] K. Englehart, B. Hudgins, and P. A. Parker, "A wavelet-based continuous classification scheme for multifunction myoelectric control," *IEEE Trans. Biomed. Eng.*, vol. 48, no. 3, pp. 302–311, Mar. 2001.
- [18] A. D. C. Chan and G. C. Green, "Myoelectric control development toolbox," presented at the 30th Conf. Can. Med. Biol. Eng. Soc., Toronto, Canada, 2007, Paper M0100.
- [19] R. E. Bellman, *Adaptive Control Processes*. Princeton, NJ: Princeton Univ. Press, 1961.
- [20] K. Englehart, B. Hudgins, P. A. Parker, and M. Stevenson, "Classification of the myoelectric signal using time–frequency based representations," *Med. Eng. Phys.*, vol. 21, pp. 431–438, 1999.
- [21] A. D. C. Chan and K. Englehart, "Continuous myoelectric control for powered prostheses using hidden Markov models," *IEEE Trans. Biomed. Eng.*, vol. 52, no. 1, pp. 121–124, Jan. 2005.
- [22] F. H. Y. Chan, Y.-S. Yang, F. K. Lam, Y.-T. Zhang, and P. A. Parker, "Fuzzy EMG classification for prosthesis control," *IEEE Trans. Rehabil. Eng.*, vol. 8, no. 3, pp. 305–311, Sep. 2000.
- [23] R. F. ff. Weir and A. B. Ajiboye, "A multifunction prosthesis controller based on fuzzy-logic techniques," in *Proc. 25th Silver Anniv. Int. Conf. IEEE Eng. Med. Biol. Soc.*, Cancun, Mexico, Sep. 17–21, 2003, pp. 1678–1681.
- [24] K. A. Farry, J. J. Fernandez, R. Abramczyk, M. Novy, and D. Atkins, "Applying genetic programming to control of an artificial arm," in *Proc. Myoelectric Control (MEC 1997) Conf.*, Fredericton, NB, Canada, Jul. 23–25, 1997, pp. 50–55.
- [25] L. Hargrove, P. Zhou, K. Englehart, and T. Kuiken, "The effect of ECG interference on pattern recognition based myoelectric control for targeted muscle reinnervated subjects," *IEEE Trans. Biomed. Eng.*, to be published.
- [26] A. Hyvarinen, E. Oja, and J. Karhunen, *Independent Component Analysis*. New York: Wiley, 2001.
- [27] X. Liu, T. Chen, and B. V. K. Kumar, "Face authentication for multiple subjects using Eigenflow," *Pattern Recognit.*, vol. 36, pp. 313–328, 2003.
- [28] K. Vanketaramani, S. Qidwai, and B. Vijayakumar, "Face authentication from cell phone camera images with illumination and temporal variations," *IEEE Trans. Syst., Man, Cybern.*, vol. 35, no. 3, pp. 411–418, Aug. 2005.
- [29] K. Das, S. Osechinskiy, and Z. Nenadic, "A classwise PCA-based recognition of neural data for brain computer interfaces," in *Proc. 29th Annu. Int. Conf. IEEE Eng. Med. Biol. Soc.*, Lyon, France, 2007, pp. 6519–6522.
- [30] P. Somol, P. Pudil, J. Novovicova, and P. Paclik, "Adaptive floating search methods in feature selection," *Pattern Recognit. Lett.*, vol. 20, pp. 1157–1163, 1999.
- [31] S. Micera, A. Sabatini, P. Dario, and B. Rossi, "A hybrid approach to EMG pattern analysis using statistical and fuzzy techniques," *Med. Eng. Phys.*, vol. 21, pp. 303–311, 1999.
- [32] O. Fukuda, T. Tsuji, M. Kaneko, and A. Otsuka, "A human-assisting manipulator teleoperated by EMG Signals and arm motions," *IEEE Trans. Robot. Autom.*, vol. 19, no. 2, pp. 210–222, Apr. 2003.
- [33] T. Farrell and R. F. Weir, "The optimal controller delay for myoelectric prostheses," *IEEE Trans. Neurosci. Rehabil. Eng.*, vol. 15, no. 1, pp. 111–118, Mar. 2007.



Levi J. Hargrove (S'05–M'09) received the B.Sc., M.Sc., and Ph.D. degrees in electrical engineering from the University of New Brunswick (UNB), Fredericton, NB, Canada, in 2003, 2005, and 2008, respectively.

He is currently a Research Engineer with the Neural Engineering Center for Artificial Limbs at the Rehabilitation Institute of Chicago, and is an Assistant Research Professor in the Department of Physical Medicine and Rehabilitation at Northwestern University, Chicago, IL. His current research interests include neuromuscular modeling biological signal processing, and pattern-recognition-based control for myoelectric prostheses.

Dr. Hargrove is also a Registered Professional Engineer.



Guanglin Li (M'01–SM'06) received the B.S. and M.S. degrees in electrical engineering from Shandong University, Jinan, China, in 1983 and 1988, respectively, and the Ph.D. degree in biomedical engineering from Zhejiang University, Hangzhou, China, in 1997.

In 1997, he joined the Department of Electrical Engineering, Shandong University, where he became an Associate Professor in 1998. During 1999–2002, he was a Research Fellow, and later, a Postdoctoral Research Associate in the Department of Bioengineering, University of Illinois at Chicago. From 2002 to 2005, he was a Senior Research Scientist at BioTechPlex Corporation. From 2006 to 2008, he was with the Rehabilitation Institute of Chicago, Chicago, where he was a Senior Research Scientist in the Neural Engineering Center for Artificial Limbs and with the Northwestern University, Chicago, where he was a Research Assistant Professor of physical medicine and rehabilitation. Since 2009, he has been with Shenzhen Institute of Advanced Technology, Chinese Academy of Sciences, China, where he is currently a Professor. His current research interests include neuroprosthesis, neural–machine interface, biomedical signal analysis, and computational biomedical engineering.



Kevin B. Englehart (S'86–M'99–SM'03) received the B.Sc. degree in electrical engineering and the M.Sc. and Ph.D. degrees from the University of New Brunswick (UNB), Fredericton, NB, Canada, in 1989, 1992, and 1998, respectively.

He is currently a Professor of electrical and computer engineering, UNB, where he is also the Associate Director of the Institute of Biomedical Engineering. His current research interests include neuromuscular modeling and biological signal processing using adaptive systems, pattern recognition,

and time–frequency analysis.

Dr. Englehart is a Registered Professional Engineer. He is also a member of the IEEE Engineering in Medicine and Biology Society, the IEEE Computer Society, and the Canadian Medical and Biological Engineering Society.



Bernard S. Hudgins (M'97–SM'01) received the Ph.D. degree from the University of New Brunswick (UNB), Fredericton, NB, Canada, in 1991.

He is currently the Director of the Institute of Biomedical Engineering, UNB, where he is also a Professor of electrical and computer engineering. His current research interests include the areas of myoelectric signal processing for the control of artificial limbs and rehabilitation engineering. He has recently spent two years on a North Atlantic Treaty Organization (NATO) workgroup assessing alternative control

technologies for cockpit applications.

Prof. Hudgins was the recipient of a Whitaker Foundation Young Investigator Award. He has also been a Region 7 (Canada) representative on the IEEE Engineering in Medicine and Biology Society (EMBS) Advisory Committee and the IEEE EMBS Vice President for Publications and Technical Activities.